

**Conductance enhancement due to interface magnons in electron-beam evaporated MgO magnetic tunnel junctions with CoFeB free layer deposited at different pressure**

P. Guo, D. L. Li, J. F. Feng, H. Kurt, G. Q. Yu, J. Y. Chen, H. X. Wei, J. M. D. Coey, and X. F. Han

Citation: [Journal of Applied Physics](#) **116**, 153905 (2014); doi: 10.1063/1.4898683

View online: <http://dx.doi.org/10.1063/1.4898683>

View Table of Contents: <http://scitation.aip.org/content/aip/journal/jap/116/15?ver=pdfcov>

Published by the [AIP Publishing](#)

---

**Articles you may be interested in**

[Inelastic tunneling conductance and magnetoresistance investigations in dual ion-beam sputtered CoFeB\(110\)/MgO/CoFeB \(110\) magnetic tunnel junctions](#)

[J. Appl. Phys.](#) **115**, 153903 (2014); 10.1063/1.4871679

[Giant tunneling magnetoresistance with electron beam evaporated MgO barrier and CoFeB electrodes](#)

[J. Appl. Phys.](#) **107**, 083920 (2010); 10.1063/1.3371811

[Temperature dependence of tunnel resistance for Co Fe B/Mg O/Co Fe B magnetoresistive tunneling junctions: The role of magnon](#)

[J. Appl. Phys.](#) **101**, 09B504 (2007); 10.1063/1.2712322

[Tunneling spectroscopy in CoFeB/MgO/CoFeB magnetic tunnel junctions](#)

[J. Appl. Phys.](#) **99**, 08A905 (2006); 10.1063/1.2173628

[Inelastic tunneling spectroscopy of magnetic tunnel junctions based on CoFeB/MgO/CoFeB with Mg insertion layer](#)




[J. Appl. Phys.](#) **99**, 08T305 (2006); 10.1063/1.2162047

---



**AIP** | Journal of Applied Physics

**Meet The New Deputy Editors**

	<b>Christian Brosseau</b>		<b>Laurie McNeil</b>		<b>Simon Phillpot</b>
---	---------------------------	---	----------------------	---	-----------------------

# Conductance enhancement due to interface magnons in electron-beam evaporated MgO magnetic tunnel junctions with CoFeB free layer deposited at different pressure

P. Guo,<sup>1</sup> D. L. Li,<sup>1,2</sup> J. F. Feng,<sup>1,2,a)</sup> H. Kurt,<sup>2,3</sup> G. Q. Yu,<sup>1</sup> J. Y. Chen,<sup>2</sup> H. X. Wei,<sup>1</sup>  
 J. M. D. Coey,<sup>2</sup> and X. F. Han<sup>1,a)</sup>

<sup>1</sup>Beijing National Laboratory of Condensed Matter Physics, Institute of Physics, Chinese Academy of Sciences, Beijing 100190, China

<sup>2</sup>CRANN and School of Physics, Trinity College, Dublin 2, Ireland

<sup>3</sup>Department of Engineering Physics, Istanbul Medeniyet University, 34720 Istanbul, Turkey

(Received 23 July 2014; accepted 8 October 2014; published online 17 October 2014)

Electron-beam evaporated MgO-based magnetic tunnel junctions have been fabricated with the CoFeB free layer deposited at Ar pressure from 1 to 4 mTorr, and their tunneling process has been studied as a function of temperature and bias voltage. By changing the growth pressure, the junction dynamic conductance  $dI/dV$ , inelastic electron tunneling spectrum  $d^2I/dV^2$ , and tunneling magnetoresistance vary with temperature. Moreover, the low-energy magnon cutoff energy  $E_C$  derived from the conductance versus temperature curve agrees with interface magnon energy obtained directly from the inelastic electron tunneling spectrum, which demonstrates that interface magnons are involved in the electron tunneling process, opening an additional conductance channel and thus enhancing the total conductance. © 2014 AIP Publishing LLC.

[<http://dx.doi.org/10.1063/1.4898683>]

## INTRODUCTION

Magnetic tunnel junctions (MTJs) with the core structure of an insulating layer sandwiched between two ferromagnetic layers have the potential to be widely used as the key element in read heads of hard disk drives,<sup>1</sup> magnetic sensors,<sup>2,3</sup> magnetic random access memory (MRAM),<sup>4,5</sup> and magnetic logic devices.<sup>6,7</sup> Compared with AlO<sub>x</sub>-based MTJs,<sup>8–11</sup> MgO-based MTJs prepared by magnetron sputtering<sup>12,13</sup> or molecular beam epitaxy (MBE)<sup>14</sup> have a higher tunneling magnetoresistance (TMR) ratio originating from spin-filtering effect<sup>15,16</sup> of high quality MgO (001) barrier. Some of us have recently demonstrated that electron-beam (EB) evaporated MgO grown on amorphous CoFeB shows a good (001) texture and its lattice matches well with crystallized CoFeB,<sup>17–20</sup> which results in a TMR of EB-MgO MTJs comparable to that of MTJs with MgO barriers deposited by RF sputtering or MBE. When an electron tunnels from one ferromagnetic electrode to the other electrode in a MTJ, a magnon is probable to be emitted or absorbed, opening up a new conductance channel and enhancing the total conductance.<sup>21,22</sup> Therefore, verifying the existence of interface magnons and determining their energy is a research concern.<sup>21–24</sup>

The growth conditions of MgO tunnel barrier in MTJs have a strong influence on TMR and noise parameters,<sup>25–28</sup> but there are fewer reports about the influence of the growth conditions on ferromagnetic electrode, which is possible to affect TMR and the tunneling process of MTJs. In this work, we have grown EB-MgO MTJs, with CoFeB free layer at different Ar pressures, to investigate the influence of CoFeB deposition conditions on the magnetoelectric transport properties.

Tunneling resistances in both parallel (P) and antiparallel (AP) states were measured at different temperatures ( $T$ ), and the dynamic conductance  $dI/dV$  and inelastic electron tunneling spectrum  $d^2I/dV^2$  at low temperature were simultaneously obtained using two lock-in amplifiers to reveal the elastic and inelastic electron tunneling processes in these MTJs.

## EXPERIMENT

All MTJ stacks with the structure of Ta (5)/Ru (30)/Ta (5)/Ni<sub>81</sub>Fe<sub>19</sub> (5)/Ir<sub>22</sub>Mn<sub>78</sub> (10)/Co<sub>90</sub>Fe<sub>10</sub> (2.5)/Ru (0.9)/Co<sub>40</sub>Fe<sub>40</sub>B<sub>20</sub> (3) (1 mTorr)/MgO (2.5)/Co<sub>40</sub>Fe<sub>40</sub>B<sub>20</sub> (3) (1, 2, 3, 4 mTorr)/Ta (5)/Ru (5) (all thicknesses in nanometers) were deposited on thermally oxidized Si wafers. The active structure Co<sub>40</sub>Fe<sub>40</sub>B<sub>20</sub> (3) (1 mTorr)/MgO (2.5)/Co<sub>40</sub>Fe<sub>40</sub>B<sub>20</sub> (3) (1, 2, 3, 4 mTorr) was deposited in a vacuum chamber with a base pressure of  $2.1 \times 10^{-10}$  Torr (1 Torr = 1000 mTorr = 133 Pa). It is noteworthy that the bottom CoFeB electrode was sputtered at 1 mTorr Ar pressure, while the top electrode was deposited at Ar pressures of 1, 2, 3, or 4 mTorr. With increasing Ar pressure from 1 to 4 mTorr, the CoFeB deposition rate decreases from  $0.04 \pm 0.001$  to  $0.03 \pm 0.001$  nm/s. MgO barrier was electron-beam evaporated from MgO sintered target in the same UHV chamber. Other metallic layers were DC sputtered by transferring the sample into an adjacent vacuum chamber in the modified Shamrock deposition tool having a base pressure of  $1 \times 10^{-7}$  Torr. The stacks were then patterned into junctions with the dimension of  $5 \times 10 \mu\text{m}^2$  using ultraviolet (UV) lithography and Ar ion beam milling, and annealed in an in-plane field of 8000 Oe (1 T =  $10^4$  Oe) at 350 °C for 30 min to define the exchange bias of the antiferromagnetic layer and improve the quality of the MgO/CoFeB interfaces. A Quantum Design Physical

<sup>a)</sup>Authors to whom correspondence should be addressed. Electronic addresses: jiafengfeng@aphy.iphy.ac.cn and xfhan@aphy.iphy.ac.cn.

Properties Measurement System (PPMS) combined with conventional four-terminal method with DC voltage of 5 mV was used to measure the magnetoelectric transport properties. The standard lock-in method with AC modulation of 4 mV and frequency of 30.79 Hz was utilized to obtain the dynamic conductance  $dI/dV$  and inelastic electron tunneling spectroscopy (IETS)  $d^2I/dV^2$  at 10 K.

## RESULTS AND DISCUSSION

Fig. 1 shows typical  $R$  versus  $H$  curves for MTJs with the CoFeB free layer deposited at different Ar pressures at 300 K and 10 K, respectively. Compared with 300 K,  $R_P$  (resistance in the parallel configuration) at 10 K, only increases a little in all MTJs. By contrast, the variation of  $R_{AP}$  (resistance in the antiparallel configuration) is substantial. TMR at 300 K for these MTJs are 267%, 286%, 242%, and 228%, respectively, and increases up to 393%, 431%, 374%, and 356% when temperature is reduced to 10 K. Compared with 300 K, thermal excitation at 10 K is negligible, thus causing both  $R_P$  and  $R_{AP}$  to increase, while weakened magnetic disorder makes  $R_P$  decrease but  $R_{AP}$  increase. Therefore, the values of  $R_P$  and  $R_{AP}$  at 300 K and 10 K are a result of competing thermal excitation and magnetic disorder. As shown in Fig. 1, upon increasing Ar pressure from 1 to

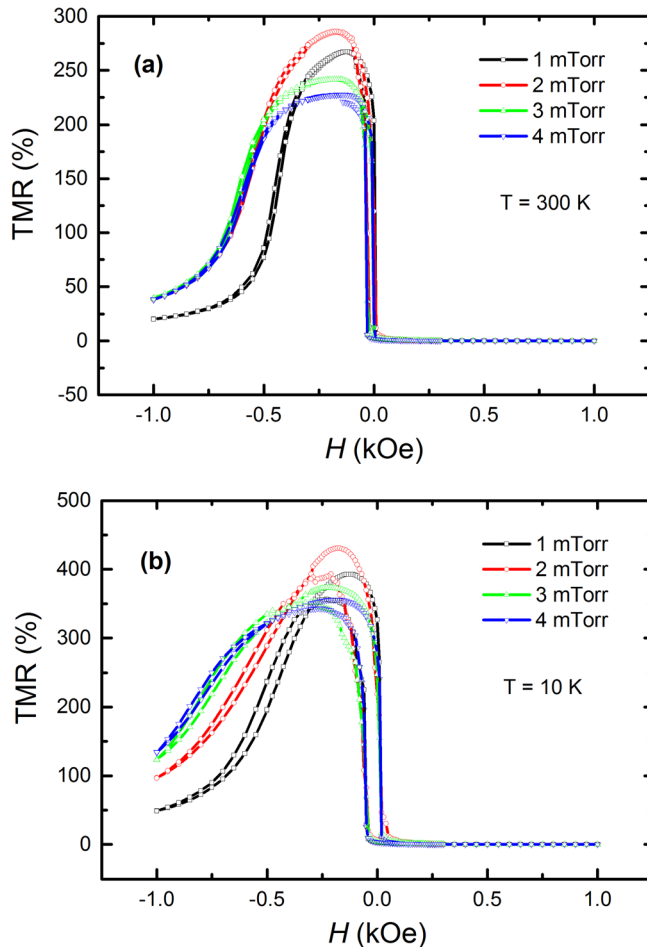


FIG. 1. Typical  $R$  versus  $H$  curves at 300 K (a) and 10 K (b) for MTJs with the CoFeB free layer grown at Ar pressures of 1, 2, 3, and 4 mTorr, respectively.

4 mTorr, TMR at 300 K has a tendency to decrease from 267% to 228%, probably due to the rougher CoFeB/MgO top interface at higher deposition pressure, which causes target atoms to have lower surface mobility.<sup>26</sup>

Coercivity  $H_C$  versus temperature obtained from  $R(H)$  loops at different temperatures is plotted in Fig. 2.  $H_C$  for MTJs with CoFeB free layers deposited at different Ar pressures at 300 K is about 15 Oe, which increases to about 40 Oe at 2 K. On decreasing temperature from 300 K to 2 K,  $H_C$  for these MTJs is almost doubled due to the progressive reduction of the thermal excitations, and thus a larger magnetic field is needed to switch the CoFeB free layer. In addition,  $H_C$  shows little Ar pressure dependence since it is a bulk rather than an interfacial property.

Fig. 3 shows the temperature dependence of  $R_P$ ,  $R_{AP}$ , and the TMR ratio. With decreasing temperature from 300 K to 2 K,  $R_P$  for MTJs with the CoFeB free layer grown at different Ar pressures shows weak temperature dependence, and increases only slightly, while  $R_{AP}$  for these MTJs increases significantly, by about 50%, thus clearly enhancing TMR from 286% to 420% for a MTJ grown at an Ar pressure of 2 mTorr as an example. According to the models developed by Zhang *et al.*<sup>21</sup> and Wei *et al.*,<sup>24</sup> the conductance  $G$  at temperature  $T$  and bias voltage  $V$  can be expressed as

$$G^\gamma(T, V) = G_{\text{direct}}^\gamma(0, V) + G_{\text{magnon}}^\gamma(T, V), \quad (1)$$

$$G_{\text{magnon}}^\gamma(T, V) = C \left[ -2k_B T \ln(1 - e^{-E_C/k_B T}) + \frac{|eV| + E_C}{e^{(|eV| + E_C)/k_B T} - 1} + \frac{|eV| - E_C}{1 - e^{-(|eV| - E_C)/k_B T}} \right], \quad (2)$$

where  $\gamma = (P, AP)$  in Eqs. (1) and (2) represents parallel (P) and antiparallel (AP) configurations, respectively; the first and second terms in Eq. (1) are direct elastic tunneling conductance and magnon-assisted inelastic tunneling conductance, respectively;  $C$  in Eq. (2) is related to the spin and Curie temperature of the ferromagnetic electrode;  $E_C$  in

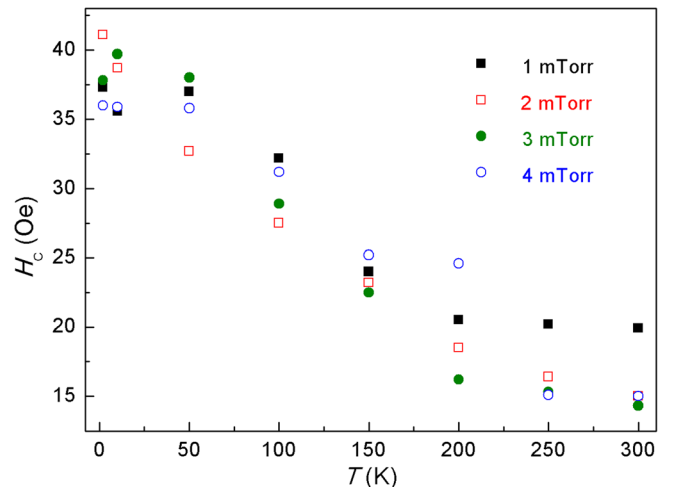


FIG. 2. Temperature dependence of coercivity  $H_C$  for MTJs with the CoFeB free layer deposited at different Ar pressures from 1 to 4 mTorr.

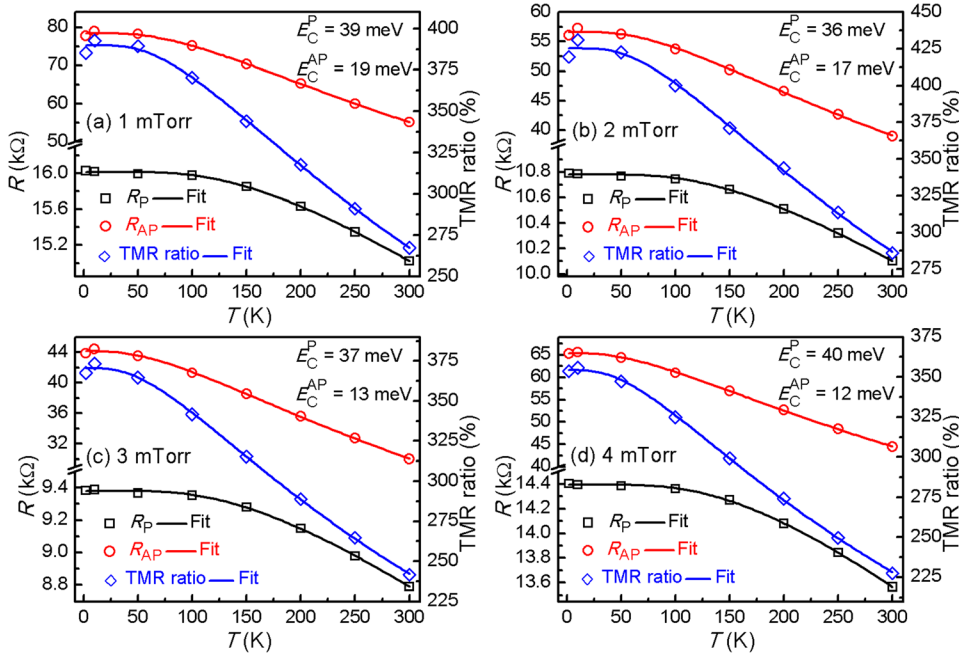


FIG. 3. Temperature dependence of  $R_p$ ,  $R_{AP}$ , and the TMR ratio for MTJs with the CoFeB free layer growth pressure of (a) 1, (b) 2, (c) 3, and (d) 4 mTorr. Solid lines are fits based on Wei's model (Ref. 24).

Eq. (2) denotes the low-energy magnon cutoff energy. Note that a constant voltage of 5 mV is used when the  $R(H)$  loop is measured, so  $V$  is fixed at 5 mV to fit the data. The measured  $R_p$ ,  $R_{AP}$ , and TMR ratio can be well fitted using Eqs. (1) and (2). The most important fitting parameter for these MTJs is  $E_C$ ; its values are shown in Fig. 5.  $E_C$  results to be about 36 meV for the P configuration and 15 meV for the AP configuration.

The dynamic conductance  $dI/dV$  and IETS for MTJs with CoFeB free layer grown at Ar pressure from 1 to

4 mTorr are plotted in Fig. 4. Generally, three peaks can be clearly seen in MgO-based MTJs—the zero-bias anomaly (ZBA) at voltages lower than 15 mV originating from magnetic impurities, a magnon peak (M) between 20 mV and 35 mV due to interface magnons, and a phonon peak (Ph) at about 81 mV due to barrier phonons.<sup>29,30</sup> In the P-state dynamic conductance, ZBA, M, and Ph appear at 0, 20, and 88 mV, respectively, while only the ZBA at 0 mV is visible in the AP state. In addition, in the P-state dynamic conductance, a dip located at 335 mV and marked with D is possibly

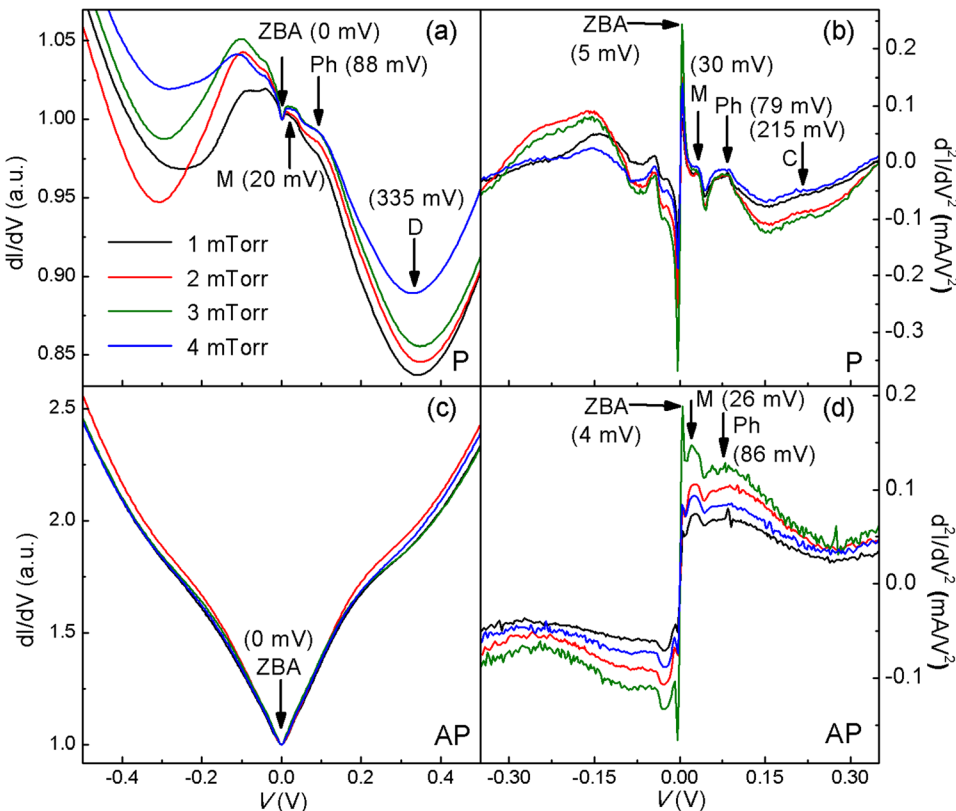


FIG. 4. Dynamic conductance  $dI/dV$  in the P (a) and AP (c) states, and IETS in the P (b) and AP (d) states for MTJs with the CoFeB free layer growth pressure from 1 to 4 mTorr. ZBA, M, and Ph mark the positions of zero-bias anomaly (ZBA), interface magnon (M), and barrier phonon (Ph), respectively. D labels the minimum conductance coming from the band structure of ferromagnetic electrode, while C is a characteristic peak for MTJs with a high TMR ratio.

from the electronic energy band structure of ferromagnetic electrode, considering that the top of the majority spin  $\Delta_2'$  and  $\Delta_5$  bands for Fe lie 0.2 eV above Fermi level  $E_F$  and the top of minority spin  $\Delta_2$  band for Co lies 0.3 eV above  $E_F$ ,<sup>31,32</sup> so the conduction channel of the state for crystallized CoFeB is closed if the energy of electrons is over the top of the bands mentioned above, thus causing minimum conductance at D. By contrast, in the P (AP)-state IETS, ZBA, M, and Ph are located at 5 mV (4 mV), 30 mV (26 mV), and 79 mV (86 mV), respectively. Additionally, a small peak labeled with C is at 215 mV in P-state IETS, which is considered as a characteristic peak for MTJs with high TMR ratio.<sup>30</sup> It is noteworthy that the characteristic peak or dip positions are independent of CoFeB free layer growth pressure.

The low-energy magnon cutoff energy  $E_C$  deduced from the fitting of  $R_{P,AP}$  versus  $T$  curves using Wei's model<sup>24</sup> and the interface magnon energy directly retrieved from IETS are summarized in Fig. 5.  $E_C$  is close to the interface magnon energy in both P and AP configurations, indicating that interface magnons are indeed involved in the tunneling process, thereby enhancing conductance, see the feature peak M in Fig. 4(a).  $E_C$  or energy of interface magnon in the P state is larger than that in the AP state, indicating that low-energy magnon cutoff energy or interface magnon energy depends strongly on the magnetic configurations of these MTJs and the AP state is more active for magnon excitations. Moreover,  $E_C$  in the P state is weakly dependent on the growth pressure of CoFeB free layer, but it decreases clearly in the AP state with increasing growth pressure from 1 to 4 mTorr, possibly owing to the rougher interface at higher growth pressure.<sup>26</sup> Moreover, compared to TMR,  $E_C$  in the AP state has a similar change as a function of the free layer growth pressure. It may indicate that MTJs with a rougher MgO/CoFeB interface have a lower  $E_C$  value, which is easy to induce magnon excitations at low temperatures and usually destroys the TMR effect as mentioned above.

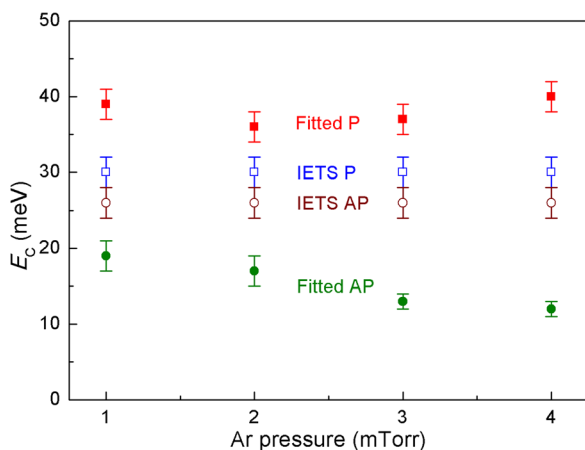


FIG. 5. The CoFeB free layer growth pressure dependence of low-energy magnon cutoff energy  $E_C$  deduced from  $R_{P,AP}(T)$  curves and interface magnon energy directly obtained from IETS of MTJs for both P and AP configurations.

## CONCLUSIONS

In conclusion, MTJs with an MgO barrier prepared by electron beam evaporation and a CoFeB free layer sputtered with Ar pressure varying from 1 to 4 mTorr have been investigated. Upon increasing the deposition pressure from 1 to 4 mTorr, TMR tends to decrease from 267% to 228%, possibly owing to the rougher CoFeB/MgO top interface at higher deposition pressure.  $R_P$  only increases a little with decreasing temperature, indicating the quality of MgO grown by electron beam evaporation is high, while the increase of  $R_{AP}$  is substantial, therefore resulting in the significant increase of TMR.  $H_C$  also increases from about 15 Oe at 300 K to 40 Oe at 2 K originating from the progressive reduction of the thermal excitations. ZBA, M, and Ph are clearly visible in the P-state  $dI/dV$ , and both P- and AP-state IETS, while only ZBA is obvious in the AP-state  $dI/dV$ . Besides, a feature marked C is observed and identified as a characteristic of MTJs with high quality MgO. The low-energy magnon cutoff energy  $E_C$  deduced from the fitting result of  $R_{P,AP}(T)$  curves agrees with interface magnon energy directly obtained from IETS, confirming that interface magnons do participate in the electron tunneling process, opening a new conductance channel and enhancing the total conductance. In addition,  $E_C$  in the P state is larger than that in the AP state and  $E_C$  in the P state decreases with the increase of CoFeB free layer deposition pressure, probably due to the rougher interface at higher growth pressure, showing that  $E_C$  is dependent on both ferromagnetic electrode growth pressure and magnetic configuration of the MTJs.

## ACKNOWLEDGMENTS

The work was supported by the State Key Project of Fundamental Research of Ministry of Science and Technology [MOST, No. 2010CB934400], the National Natural Science Foundation [NSFC, Grant Nos. 11374351, 11174341, and 11222432], and Science Foundation Ireland via the NISE project 10/IN.1/13006.

<sup>1</sup>J. G. Zhu and C. Park, *Mater. Today* **9**, 36 (2006).

<sup>2</sup>B. Negulescu, D. Lacour, F. Montaigne, A. Gerken, J. Paul, V. Spetter, J. Marien, C. Duret, and M. Hehn, *Appl. Phys. Lett.* **95**, 112502 (2009).

<sup>3</sup>J. Y. Chen, J. F. Feng, and J. M. D. Coey, *Appl. Phys. Lett.* **100**, 142407 (2012).

<sup>4</sup>S. S. P. Parkin, K. P. Roche, M. G. Samant, P. M. Rice, R. B. Beyers, R. E. Scheuerlein, E. J. O'Sullivan, S. L. Brown, J. Bucchigano, D. W. Abraham, Y. Lu, M. Rooks, P. L. Trouilloud, R. A. Wanner, and W. J. Gallagher, *J. Appl. Phys.* **85**, 5828 (1999).

<sup>5</sup>E. Chen, D. Apalkov, Z. Diao, A. Driskill-Smith, D. Druist, D. Lottis, V. Nikitin, X. Tang, S. Watts, S. Wang, S. A. Wolf, A. W. Ghosh, J. W. Lu, S. J. Poon, M. Stan, W. H. Butler, S. Gupta, C. K. A. Mewes, T. Mewes, and P. B. Visscher, *IEEE Trans. Magn.* **46**, 1873 (2010).

<sup>6</sup>A. Ney, C. Pampuch, R. Koch, and K. H. Ploog, *Nature* **425**, 485 (2003).

<sup>7</sup>J. G. Wang, H. Meng, and J. P. Wang, *J. Appl. Phys.* **97**, 10D509 (2005).

<sup>8</sup>J. S. Moodera, L. R. Kinder, T. M. Wong, and R. Meservey, *Phys. Rev. Lett.* **74**, 3273 (1995).

<sup>9</sup>T. Miyazaki and N. Tezuka, *J. Magn. Magn. Mater.* **139**, L231 (1995).

<sup>10</sup>S. Yuasa, T. Sato, E. Tamura, Y. Suzuki, H. Yamamori, K. Ando, and T. Katayama, *Europhys. Lett.* **52**, 344 (2000).

<sup>11</sup>T. Dimopoulos, G. Gieres, J. Wecker, Y. Luo, and K. Samwer, *Europhys. Lett.* **68**, 706 (2004).

<sup>12</sup>S. S. P. Parkin, C. Kaiser, A. Panchula, P. M. Rice, B. Hughes, M. Samant, and S.-H. Yang, *Nature Mater.* **3**, 862 (2004).

- <sup>13</sup>D. D. Djayaprawira, K. Tsunekawa, M. Nagai, H. Maehara, S. Yamagata, N. Watanabe, S. Yuasa, Y. Suzuki, and K. Ando, *Appl. Phys. Lett.* **86**, 092502 (2005).
- <sup>14</sup>S. Yuasa, T. Nagahama, A. Fukushima, Y. Suzuki, and K. Ando, *Nature Mater.* **3**, 868 (2004).
- <sup>15</sup>W. H. Butler, X.-G. Zhang, T. C. Schulthess, and J. M. MacLaren, *Phys. Rev. B* **63**, 054416 (2001).
- <sup>16</sup>J. Mathon and A. Umerski, *Phys. Rev. B* **63**, 220403(R) (2001).
- <sup>17</sup>H. Kurt, K. Oguz, T. Niizeki, and J. M. D. Coey, *J. Appl. Phys.* **107**, 083920 (2010).
- <sup>18</sup>Z. Diao, J. F. Feng, H. Kurt, G. Feng, and J. M. D. Coey, *Appl. Phys. Lett.* **96**, 202506 (2010).
- <sup>19</sup>H. Kurt, K. Rode, K. Oguz, M. Boese, C. C. Faulkner, and J. M. D. Coey, *Appl. Phys. Lett.* **96**, 262501 (2010).
- <sup>20</sup>J. F. Feng, Z. Diao, H. Kurt, R. Stearrett, A. Singh, E. R. Nowak, and J. M. D. Coey, *J. Appl. Phys.* **112**, 093913 (2012).
- <sup>21</sup>V. Drewello, J. Schmalhorst, A. Thomas, and G. Reiss, *Phys. Rev. B* **77**, 014440 (2008).
- <sup>22</sup>H. X. Wei, Q. H. Qin, Q. L. Ma, X.-G. Zhang, and X. F. Han, *Phys. Rev. B* **82**, 134436 (2010).
- <sup>23</sup>S. Zhang, P. M. Levy, A. C. Marley, and S. S. P. Parkin, *Phys. Rev. Lett.* **79**, 3744 (1997).
- <sup>24</sup>X. F. Han, A. C. C. Yu, M. Oogane, J. Murai, T. Daibou, and T. Miyazaki, *Phys. Rev. B* **63**, 224404 (2001).
- <sup>25</sup>S. Ikeda, J. Hayakawa, Y. M. Lee, R. Sasaki, T. Meguro, F. Matsukura, and H. Ohno, *Jpn. J. Appl. Phys., Part 2* **44**, L1442 (2005).
- <sup>26</sup>W. F. Shen, D. Mazumdar, X. J. Zou, X. Y. Liu, B. D. Schrag, and G. Xiao, *Appl. Phys. Lett.* **88**, 182508 (2006).
- <sup>27</sup>A. Zaleski, J. Wrona, M. Czapkiewicz, W. Skowronski, J. Kanak, and T. Stobiecki, *J. Appl. Phys.* **111**, 033903 (2012).
- <sup>28</sup>J. F. Feng, J. Y. Chen, H. Kurt, and J. M. D. Coey, *J. Appl. Phys.* **112**, 123907 (2012).
- <sup>29</sup>G.-X. Miao, K. B. Chetry, A. Gupta, W. H. Butler, K. Tsunekawa, D. Djayaprawira, and G. Xiao, *J. Appl. Phys.* **99**, 08T305 (2006).
- <sup>30</sup>V. Drewello, M. Schäfers, O. Schebaum, A. A. Khan, J. Münchenberger, J. Schmalhorst, G. Reiss, and A. Thomas, *Phys. Rev. B* **79**, 174417 (2009).
- <sup>31</sup>S. Yuasa and D. D. Djayaprawira, *J. Phys. D: Appl. Phys.* **40**, R337 (2007).
- <sup>32</sup>J. M. Teixeira, J. Ventura, M. P. Fernandez-Garcia, J. P. Araujo, J. B. Sousa, P. Wisniewski, and P. P. Freitas, *Appl. Phys. Lett.* **100**, 072406 (2012).